FLAME RETARDANT MECHANISM OF SILICA GEL/SILICA

by

Takashi Kashiwagi, Jeffrey W. Gilman, Kathryn M. Butler, Richard H. Harris, John R. Shields and Atsushi Asano
National Institute of Standards and Technology
Gaithersburg, MD 20899 USA

Reprinted from Fire and Materials, Volume 24, No. 6, 277-289, November/December 2000.

NIST
National Institute of Standards and Technology
Technology Administration, U.S. Department of Commerce

FIRE AND MATERIALS
Fire Mater. **24**, 277–289 (2000)

Flame Retardant Mechanism of Silica Gel/Silica†

Takashi Kashiwagi[1]*, Jeffrey W. Gilman[1], Kathryn M. Butler[1], Richard H. Harris[1], John R. Shields[1], Atsushi Asano[2]

[1]Materials Fire Research Group, Building and Fire Research Laboratory,
[2]Polymer Division, Materials Science and Engineering Laboratory, National Institute of Standards and Technology, Gaithersburg, MD 20899-8652, U.S.A.

Various types of silica, silica gel, fumed silicas and fused silica were added to polypropylene and polyethylene oxide to determine their flame retardant effectiveness and mechanisms. Polypropylene was chosen as a non-char-forming thermoplastic and polyethylene oxide was chosen as a polar char-forming (slight) thermoplastic. Flammability properties were measured in the cone calorimeter and the mass loss rate was measured in our radiative gasification device in nitrogen to exclude any gas phase oxidation reactions. The addition of low density, large surface area silicas, such as fumed silicas and silica gel to polypropylene and polyethylene oxide significantly reduced the heat release rate and mass loss rate. However, the addition of fused silica did not reduce the flammability properties as much as other silicas. The mechanism of reduction in flammability properties is based on the physical processes in the condensed phase instead of chemical reactions. The balance between the density and the surface area of the additive and polymer melt viscosity determines whether the additive accumulates near the sample surface or sinks through the polymer melt layer. Fumed silicas and silica gel used in this study accumulated near the surface to act as a thermal insulation layer and also to reduce the polymer concentration near the surface. However, fused silica used in this study mainly sank through the polymer melt layer and did not accumulate near the surface. The heat release and the mass loss rate of polypropylene decreased nearly proportionally with an increase in mass loading level of silica gel up to 20% mass fraction. Polyethylene oxide samples with fumed silicas and silica gel formed physically strong char/silica surface layers. This layer acted not only as thermal insulation to protect virgin polymer but also acted as a barrier against the migration of the thermal degradation products to the surface. Published in 2000 by John Wiley & Sons, Ltd.

INTRODUCTION

As an alternative to the use of halogenated flame retardants, which control flammability by modifying the gas phase chemistry in the flame,[1] our approach has been to modify the condensed phase chemistry and/or physical processes by using inorganic additives.[2–4] One such additive was a silica gel–potassium carbonate combination, which in a relatively small concentration, significantly reduced the heat release rates of various polymers.[2] It was postulated that its flame retardant mechanism occurs in the condensed phase by changing the rate of char formation relative to the rate of fuel generation supported by the higher char yield.[5] Unfortunately, potassium carbonate is hygroscopic and also relatively reactive with polymers at elevated processing temperatures. Therefore, the effect of the addition of silica gel alone (without any potassium carbonate), on the flammability properties of polypropylene, PP, (non-polar and non-charring) and polyethylene oxide, PEO, (polar and slightly char forming) is studied in this work. The effects of different types of silica and the loading level of silica gel on the flammability of PP are also determined. The flame retardant mechanism of silica gel/silica is studied by observing the gasification behaviour of the samples in a nitrogen atmosphere under external radiant flux, conducting thermal gravimetric analysis and FTIR and NMR analyses of heated sample residues, and comparing the results with the theoretically calculated sample mass loss rate in a nitrogen atmosphere.

MATERIALS

Isotactic PP having a density of 0.90 g cm^{-3} was purchased from Scientific Polymer Products, Inc‡ PEO was purchased from Aldrich Chemical Company, Inc. and its average molecular weight is 100 000. Silica gel was supplied by PQ Corporation, fumed silica was Cab-O-Sil® MS-75D, hydrophobic fumed silica (formed by a chemical reaction of fumed silica with organosilanes) was Wacker HDK H-2000, and fused silica was Siltex 44C

* Correspondence to: Dr T. Kashiwagi, Materials Fire Research Group, Building and Fire Research Laboratory, National Institute of Standards and Technology, Gaithersburg, MD 20899-8652, USA

‡Certain commercial equipment, instruments, materials, services or companies are identified in this paper in order to specify adequately the experimental procedure. This in no way implies endorsement or recommendation by NIST.

Contract/grant sponsor: Industrial Consortiun on Flame Retardant Mechanism of Silica Gel

Published in 2000 by John Wiley & Sons, Ltd.

Received 1 July 2000
25 September 2000

Table 1. Material properties of various silicas

Silica	Porosity ($cm^3 g^{-1}$)	Thermal treatment (°C, h)	Silanol surface concentration (SiOH/nm^2)	Surface area ($m^2 g^{-1}$)	Particle size (μm)
Fused silica amorphous	~0	100°C 2 h	low	low	7
Fumed silica hydrophilic	NA	None	3–4	255 ± 25	aggregate length 0.2 – 0.3
Fumed silica hydophobic[a]	NA	100°C 15 h	1–2	140 ± 30	NA
Silica gel	2.0	900°C 15 h	0.4	400 ± 40	17

from Kaopolite, Inc. Material properties of the various silicas are summarized in Table 1. These silicas are very different, specifically in terms of their particle morphology, surface area and level of silanol functionality. The fumed silicas and silica gel are very fluffy but the fused silica is dense (it feels like very fine sand). The silica gel sample with a relatively large surface area was chosen based on the results of our study to determine the effects of various silica gel characteristics such as particle size, pore volume, surface area and silanol content on the flammability properties of PP.[6] A series of experiments to study the effects of the silica type on PP and PEO was conducted with samples that were made by compression molding. However, the series to study the loading level effect of silica gel on PP was conducted with samples compounded by a twin screw extruder and then injection molded. The dimensions of all samples used in this study were 75 mm diameter and 8 mm thick.

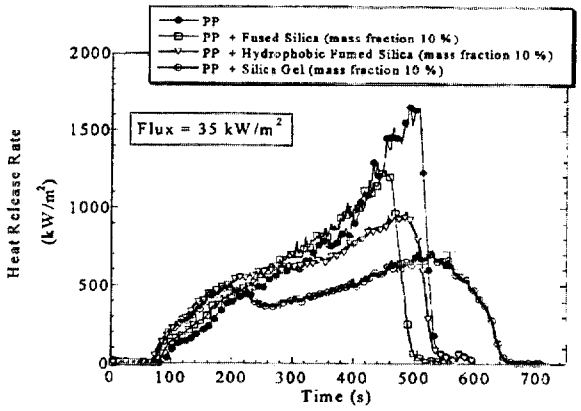

Figure 1. Effects of the addition of various silica types on the heat release rate of PP. The uncertainty in the data is shown as I.

RESULTS

Effects of the silica type on heat release rate of PP

The heat release rates and mass loss rates of the PP samples with each silica additive (except for the hydrophilic fumed silica) were measured in the cone calorimeter. The heat release rate results are shown in Fig. 1; the mass loss rate results are shown in Fig. 2. The uncertainty of these results was ± 5% due to the use of a constant heat of combustion of 13.1 $MJ kg^{-1}$ of oxygen consumption. The heat release rate and mass loss rate decreased in the following order: PP without any silica > PP with fused silica > PP with hydrophobic fumed silica > PP with silica gel. It is interesting to note that the heat release rate and the mass loss rate for PP samples containing the silica additives were slightly higher than that for pure PP shortly after ignition about 200 s. Since the heat release rate curve was very similar to the mass loss rate curve for all samples, the specific heat of combustion (heat release rate divided by mass loss rate at any instant) was about the same for the PP samples with and without the addition of the silicas. The calculated specific heat of combustion using the heat release rates with the burning mass loss rates remained constant during all tests at 42 ± 3 $MJ kg^{-1}$ for all samples. This trend indicates that the mechanism of the observed reduction in heat release rate and also in mass loss rate by the addition of the silicas depends mainly on the condensed phase process instead of the gas phase process.

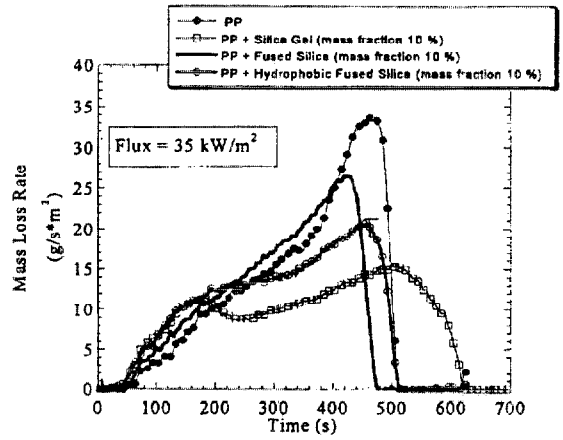

Figure 2. Effects of the addition of various silica types on the mass loss rate of PP during burning in the cone calorimeter.

Effects of the silica type on gasification rate of PP in nitrogen

The mass loss rates of pure PP and PP with the various types of silica additives (including hydrophilic fumed

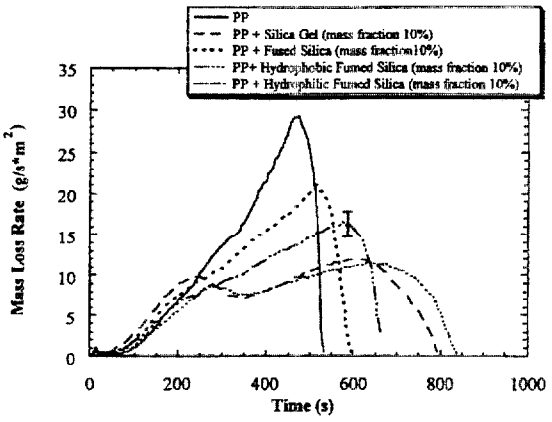

Figure 3. The effects of the addition of the various types of silicas on the mass loss rate of PP in nitrogen at the external radiant flux of 40 kW m^{-2}.

silica) were measured in a nitrogen atmosphere (no burning) under an external radiant flux of 40 kW m^{-2} in our radiative gasification device. A more detailed discussion of the device is described in our previous study.[7] The unique nature of this device is threefold: the first is that observation and the results obtained from it are only based on the condensed phase processes due to the absence of any gas phase oxidation reactions and processes; the second is to be able to visually observe gasification phenomena of a sample under the radiant flux similar to that of a fire without any interference of flame; and the third is that the external flux to the sample surface is well-defined and nearly constant over the entire experiment due to the absence of heat feedback from the flame (the slight absorption by evolved gases produces small flux variations at the sample surface[7]). The results are shown in Fig. 3. The mass loss rate decreased in the order of PP > PP with fused silica > PP with hydrophobic fumed silica > PP with either silica gel or hydrophilic silica. This trend is the same as those of the heat release rate and the mass loss rate measured in the cone calorimeter shown in Figs 1 and 2. The shape of the mass loss rate curves in Fig. 3 is very similar to those in Figs 1 and 2 including the earlier mass loss rate for the samples with silicas compared with that of pure PP. These similarities further confirm that the reduction in heat release rate and burning mass loss rate are the result of processes in the condensed phase.

Observation of the gasification of the pure PP sample first revealed melting of the sample surface at about 30 s after irradiation, followed by the appearance of several large isolated bubbles at the surface at about 60 s. Continued melting of the sample with bigger bubbles was observed at about 90 s. Vigorous bubbling started at about 120 s and the sample surface was covered by a foamy-froth of very small bubbles (very similar in appearance to that of a beer 'head') at about 180 s. This can be seen in the top left image in Fig. 4. This vigorous bubbling and froth appearance continued over the rest of the gasification experiment as seen at 300 s in the top image in Fig. 4. The sample was completely gasified without any trace of char as shown in the image at 540 s. For the sample of PP with silica gel, initial melting and bubbling phenomena were similar to the pure PP sample up to about 180 s, as seen in the left bottom picture in Fig. 4. At about 180 s, the sample surface rapidly solidified and a crust-like layer formed. It appeared that this layer continued to thicken and the production of the evolved degradation products (mass loss rate) slowed significantly, as seen in Fig. 3. It appeared that molten polymer below the crust was transported to the surface through the crust by capillary action. The mass of the residue at the end of the test (800 s) appeared to be, more or less, a crust instead of a powder, and was about 9% of the original sample mass. The surface crust layer stayed as one continuous piece until the formation of cracks when the centre portion of the crust sank near the end of the test. Although the colour of the residue was light grey, it appears that no significant amount of carbonaceous char was formed by the addition of the silica gel.

Behaviour very similar to the PP sample with silica gel was also observed for the PP sample with hydrophilic fumed silica, except that the surface layer of the residue at

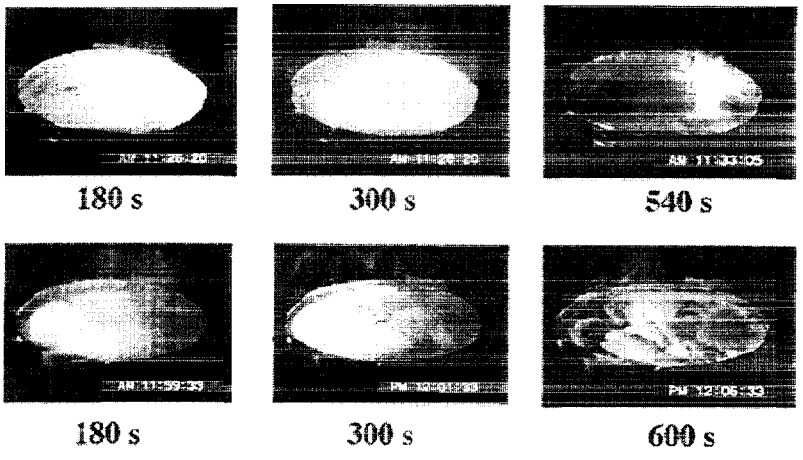

Figure 4. Selected images of the sample surface at different exposure durations during the gasification in N_2 at 40 kW m^{-2}. Pure PP (top row); PP with silica gel (bottom row).

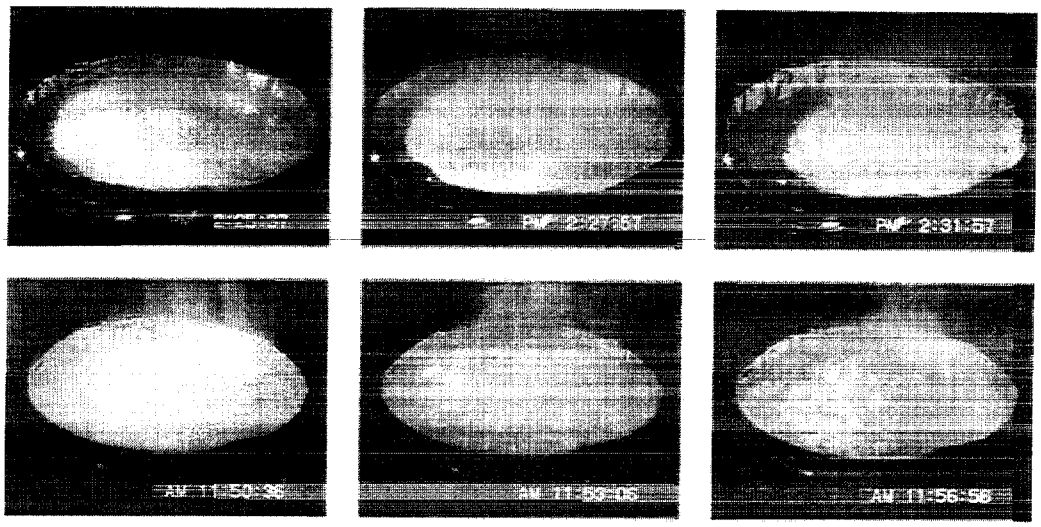

Figure 5. Selected images of gasification phenomena of PP samples in nitrogen at 40 kW m^{-2}. Top row is PP with fused silica (10% mass) and bottom row is PP with hydrophobic fumed silica (10% mass).

the end of the test was very fluffy and white. There were no cracks formed during the test. The video images of the sample of PP with fused silica showed similar bubbling phenomena to those observed for the pure PP sample up to about 200 s. At about 250 s the surface layer appeared to be slightly more viscous, and had many small bubbles bursting through a more viscous, frothy-foam surface layer. Although it appeared that silica particles accumulated on the frothy-surface, the sample behaved more or less as a fluid instead of a solid as seen in Fig. 5 (top row). This behaviour continued until about 500 s when the surface became solid-like starting at the edges and proceeding toward the centre. Scattered white powder was observed after the end of the test, and its weight was close to 10% of the original sample weight.

The digitized video images of the sample of PP with hydrophobic fumed silica are also shown in Fig. 5; however, the behaviour was similar to that of the pure PP sample up to about 200 s; i.e. with vigorous bubbling but without foaming or any frothy-foam layer. After about 200 s, the sample had large bubbles rising through a viscous layer. However, this layer still looked like a fluid. After 400 s, some solid-looking silica-covered islands were observed as seen in the image at 480 s in Fig. 5 (bottom row), and this pattern remained until close to the end of the test. Vigorous bubbling was observed between the islands.

Effects of silica gel loading level on heat release rate and gasification rate of PP

The above results show that the addition of silica gel (mass fraction of 10%) to PP produced significant reductions in heat release rate and mass loss rate. In this section, the effects of the loading level of silica gel in PP

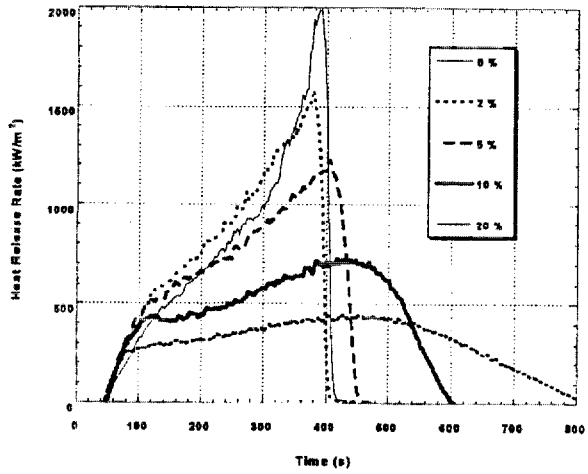

Figure 6. Effects of silica gel loading on heat release rate of PP at 40 kW m^{-2}.

on the flammability properties of PP are studied. Five PP samples with silica gel mass contents of 0%, 2%, 5%, 10% and 20% were extruded and injection molded. The heat release rates of these samples at 40 kW m^{-2} are shown in Fig. 6. The results show that the peak heat release rate of PP decreased roughly proportionally to the loading level of silica gel. However, in the period shortly after ignition, the heat release rate was slightly higher for the samples with silica gel, even with 2% mass loading, compared with that of pure PP. The duration of this higher heat release rate period was longer with a smaller loading level of silica gel; about 80% of the test time for the 2% mass loading sample, but nearly negligible for the 20% mass loading sample. The same trend

was also obtained for the burning mass loss rate shown in Fig. 7. The specific heat of combustion remained constant, $42 \pm 3\ MJ\,kg^{-1}$, during the tests and did not change with silica gel loading. The integrated heat release rate, total heat release, was about the same for all samples with or without silica gel. This indicate that, generally, the addition of silica gel tended to slow the burning process of PP.

The mass loss rates of all five samples were measured using the gasification device in nitrogen at $40\ kW\,m^{-2}$ to compare with the results obtained in the cone calorimeter and also to observe the effects of silica gel loading on gasification phenomena. The results are shown in Fig. 8. They are very similar to the results shown in Fig. 7 and again confirm that the effect of silica gel loading on the flammability of PP is based on the condensed phase process. The only difference is that the burning mass loss rates were approximately 50% higher than mass loss rates measured in nitrogen at the same external radiant flux of $40\ kW\,m^{-2}$. This difference is due to additional heat feedback of about $20\ kW\,m^{-2}$ from the flame to the sample surface in the cone calorimeter (if thermal radiation from the cone heater is significantly absorbed by the flame/combustion products, then the actual heat feedback rate would be higher than $20\ kW\,m^{-2}$).

The video images show that the sample with 2% silica gel mass loading became liquid-like with many bursting small bubbles at the surface about 100 s after the start of the irradiation and remained as a slightly viscous fluid with frequent vigorous bursting of large bubbles as seen in Fig. 9. The sample with 5% silica gel appeared to be a more viscous fluid than the 2% mass loading sample, but the overall gasification phenomena of the 5% sample were similar to that of the 2% sample until about 420 s. After 420 s, the centre part of the 5% sample appeared to become solid-like and this gradually spread toward the edges. At 650 s, the whole sample became solid-like. At this time, the mass loss rate started to decline sharply as seen in Fig. 8. For the sample with 10% silica gel, initial melting and bubbling phenomena were similar to the pure PP sample up to about 180 s, as seen in Fig. 9. At

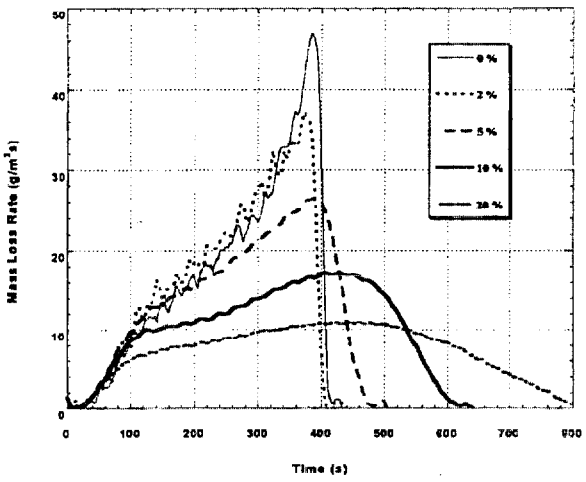

Figure 7. Effects of silica gel loading level on mass burning rate of PP at $40\ kW\,m^{-2}$.

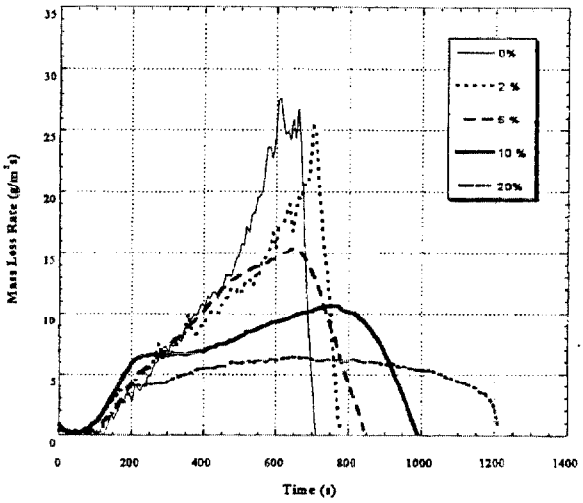

Figure 8. Effects of silica gel loading level on mass loss rate of PP in nitrogen at $40\ kW\,m^{-2}$.

about 180 s, the sample surface rapidly solidified and a crust-like layer formed. It appeared that this layer continued to thicken but large cracks appeared in the centre part of the sample at about 300 s as seen in Fig. 9. For the sample with 20% silica gel mass loading, the early melting and liquid-like behaviour, which occurred in all other samples, did not occur and the sample remained solid-like, with many cracks appearing across the crust-like surface layer at about 160 s. The crust layer with cracks remained throughout the entire test as seen in Fig. 9. Bubbling of melted polymers could be seen through the cracks. These results indicate that the mass loss rate tended to increase with time for the fluid-like melting polymer layer, but it remained relatively low when the solid-like crust surface layer was formed.

Effects of the silica type on heat release rate and mass loss rate of PEO

The difference in mass loss rates between the PP sample with hydrophilic silica and the PP sample with hydrophobic silica, as shown in Fig. 3, indicates the importance of polymer melt viscosity for flammability properties. It is known that hydrogen bonding of silica particles via surface-silanols occurs in non-polar fluids, and that in polar fluids the inter-particle hydrogen bonds are disrupted, and any thickening effect is attenuated.[8,9] Therefore, the addition of either hydrophilic fumed silica or silica gel to polar polymers may not significantly increase their melt viscosity, due to the lack of inter-particle hydrogen bonding. Since the hydrophilic silica, silica gel and hydrophobic fumed silica used in this study have relatively large surface areas as described in Table 1, it is expected that the flammability properties of PEO with these silicas would be about the same as with PP. In order to test this hypothesis, PEO was selected as the polar polymer.

The heat release rates of PEO with various types of silica are shown in Fig. 10. The results show a significant reduction of heat release rate for the PEO samples with hydrophilic and hydrophobic fumed silicas and silica gel.

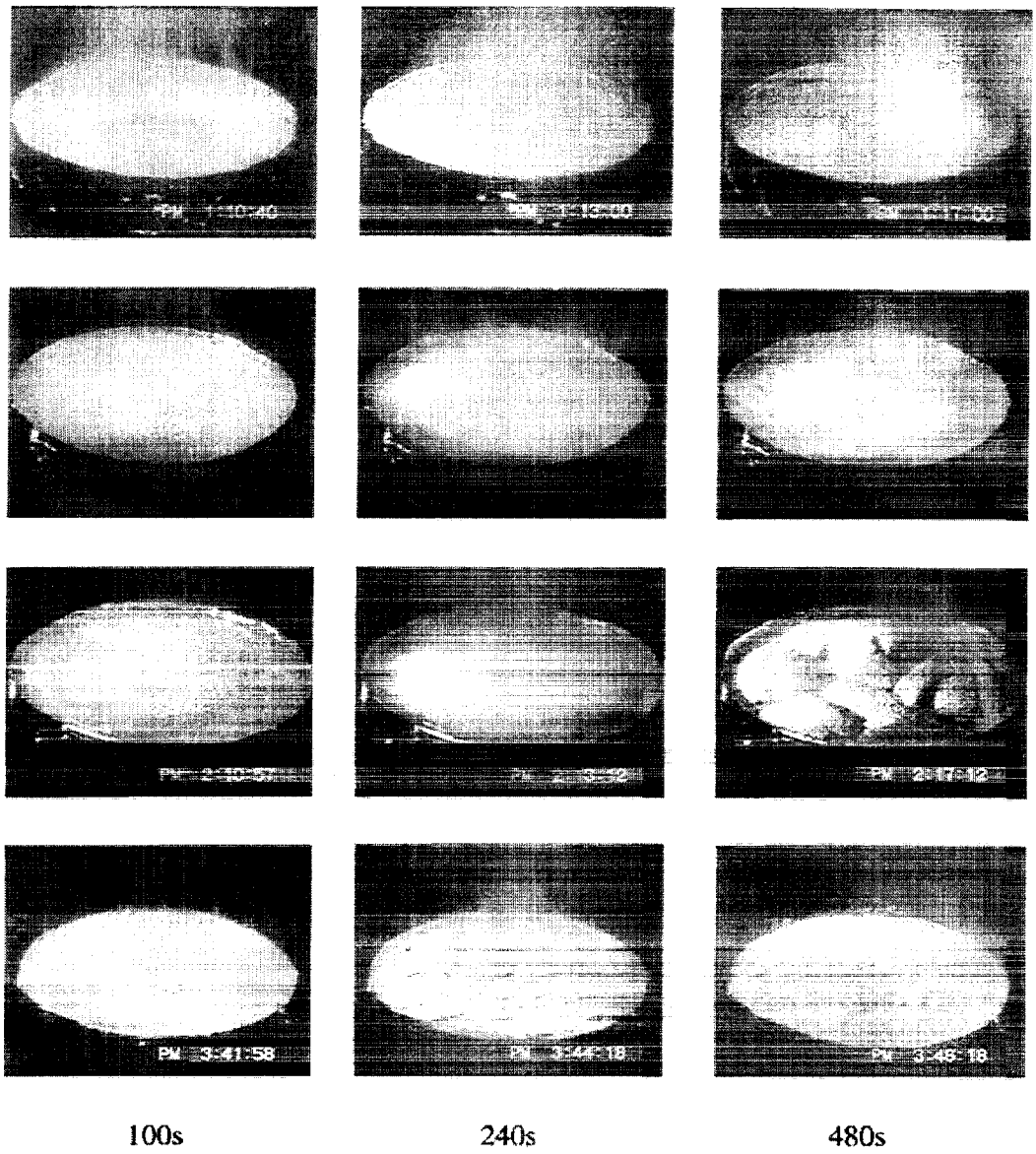

Figure 9. Effects of silica gel loading on selected video images of sample surface during gasification in nitrogen at 40 kW m^{-2}. Pure PP (top row), PP with 2% silica gel (second row), PP with 10% silica gel (third row), and PP with 20% silica gel (bottom row).

The heat release rate of the PEO sample with fused silica was not reduced as much as these three samples and this trend is similar to the PP samples with fused silica. One significant difference from the trend observed with the PP samples is that the heat release rate of the PEO sample with hydrophobic fumed silica was slightly lower than that of the PEO sample with silica gel. This clearly demonstrates that hydrogen bonding of silica particles via silanols increases polymer melt viscosity and contributes to reduce the heat release rates of non-polar PP. The burning mass loss rate curve of each PEO sample is very similar to the heat release rate curve of the corresponding sample, and thus the specific heat of combustion for all samples is about the same for all PEO samples (24 ± 2 MJ Kg^{-1}).

The mass loss rates of the above PEO samples measured in nitrogen at 40 kW m^{-2} are shown in Fig. 11. These curves are very similar to the heat release rate curves seen in Fig. 10 and they confirm that the mechanism of reduction in heat release rate by the addition of various silica types is based in the condensed phase process. The most revealing information is the observation of the gasification behaviour of the samples as seen in Fig. 12. Although PEO makes a small amount of char during gasification in nitrogen, the sample remained as a dark coloured fluid accompanied by vigorous bubbling until about 260 s. Then, a large char island emerged from the inside of the polymer melt fluid. The island repeatedly floated on the fluid surface and sank into the fluid several times until the char island grew large enough to cover

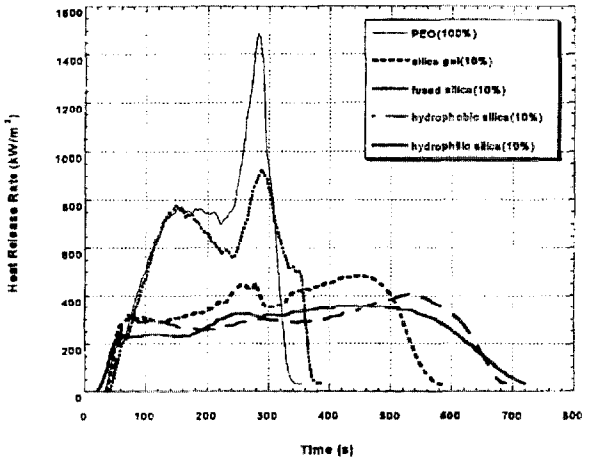

Figure 10. Effects of addition of various silica types on heat release rate of PEO at 40 kW m^{-2}.

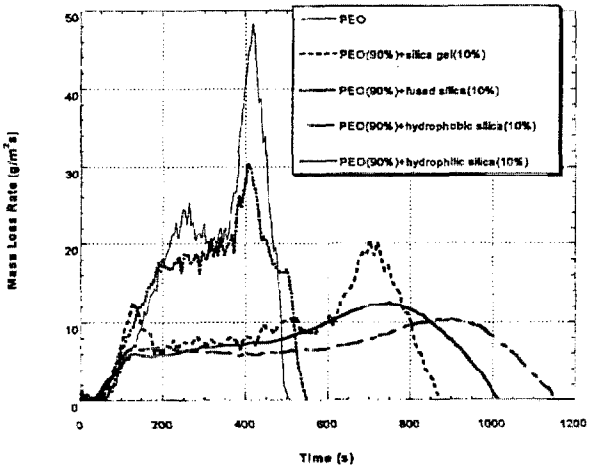

Figure 11. Effects of silica type on mass loss rate of PEO in nitrogen at 40 kW m^{-2}.

nearly the entire sample surface close to the end of the test. The addition of fused silica to PEO did not significantly change its appearance from that of pure PEO during gasification. The only noticeable change was that, once a char island was formed at about 240 s, the island gradually grew to cover the surface without sinking, but vigorous bubbling was observed where the island did not cover the sample surface. The observed reduction in the mass loss rate with fused silica compared with pure PEO was due to the partial blocking effect of the char island. The addition of fumed silicas and silica gel made a significant difference in the formation of a black, continuous, smooth solid crust surface layer at relatively early times. The black, smooth solid crust layer was formed at about 120 s for the PEO samples with fumed silicas and at about 170 s for the PEO sample with silica gel. Fluid-like behaviour accompanied by bubbling was observed for the latter sample, providing the reason for a large mass loss rate being observed up to 170 s for the PEO sample with silica gel. Several large cracks were also formed during swelling of the PEO sample with silica gel at about 420 s, and vigorous bubbling was observed through the cracks. At about 480 s, the swelling collapsed. However, no large cracks were observed for the PEO samples with fumed silicas. Cracks and the black solid crust layer could be seen in Fig. 12. These black solid crust layers consisting of char and the fumed silicas appeared to have more structural integrity than the crust layer formed over the PP samples with the same fumed silicas and silica gel.

The observed formation of the crust layer with PEO samples with both hydrophilic fumed silica and hydrophobic silica indicates that these silicas still increase the melt viscosity of polar polymers due possibly to entanglement of their polymer chains with silicas which have large surface area or large pore volume.[10]

DISCUSSION

Thermal gravimetric analysis, TGA, of the PP samples with various loading levels of silica gel was conducted to measure the thermal stability of these polymers and to determine the effect of the addition of silica gel on the thermal stability of PP. The results of derivative gravimetric analysis are shown in Fig. 13. They show that the addition of silica gel slightly increased the thermal stability of PP. The peak temperature, where the mass loss rate is the largest, increased from 444°C for the extruded PP sample without any addition of silica gel to 450°C for the PP sample with 2% mass silica gel and further to 455°C for the PP samples with 5% mass and 10% mass silica gel. However, the peak temperature decreased to 450°C for the PP sample with 20% mass silica gel. The slight increase of thermal stability might be due to the formation of tightly bound polymer chains (bounded polymer chains and their mobility is restricted) around silica particles.[11] The slight increase of thermal stability by the addition of silica gel to PP should delay the initial mass loss rate of the PP sample with the addition of silica gel. However, the observed trend of the initial mass loss rate seen in Figs 7 and 8 is slightly larger than that of pure PP. The discussion of this discrepancy will be made later in this section.

From the visual observations of the gasification experiments, as seen in Figs 4, 5 and 9, it appears that the melt viscosity of PP is significantly enhanced by the addition of silica. Both silica gel and hydrophilic fumed silica showed the same thickening behaviour, with hydrophobic fumed silica and fused silica showing only slight thickening. For the hydrophilic fumed silica the thickening was due to the inter-particle hydrogen bonding,[8] on the other hand, the thickening from silica gel can in part be due to this type of mechanism, but entanglement of the polymer in the large silica gel pores may also play a part in increasing the viscosity.[10] This indicates that the flame retardant mechanism of silicas tends to be physical in nature, instead of chemical. In order to confirm this hypothesis, residues of the PP sample with silica gel from gasification in nitrogen were collected at 300 s. This was done to examine the chemical changes in the sample during its gasification. The absorption spectra of the

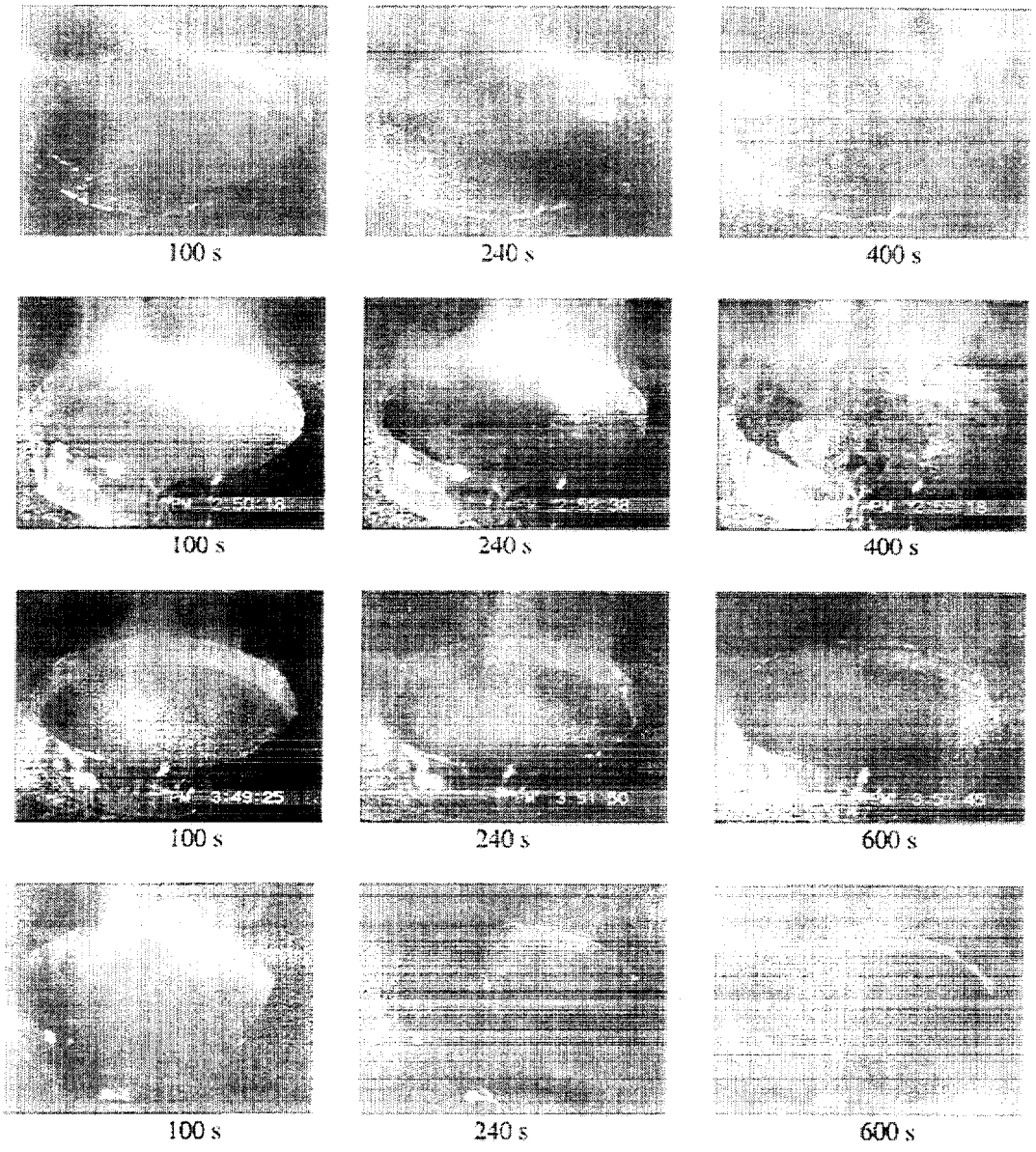

Figure 12. Selected images of gasification phenomena of PEO samples in nitrogen at 40 kW m^{-2}. Top row is PEO, the second row is PEO with fused silica (10% mass), the third row is PEO with hydrophilic fumed silica (10% mass) and bottom row is PEO with silica gel (10% mass).

original and heat-exposed samples of PP with silica gel were obtained by FTIR analysis (with KBr pellets). A comparison of the spectra for an unheated sample, and the residue from a sample irradiated in nitrogen, shown in Fig. 14, indicates that no new peaks (bonds) were formed during the gasification. Large peaks at around 1100 cm^{-1} are due to Si-O-Si stretching and the rest of the peaks are due to the PP polymer structure. A small peak near 2400 cm^{-1} in the spectra of the unheated sample is due to residual CO_2 in the chamber and this peak should be disregarded.

In the case of the PEO samples with fumed silica and silica gel, a black char-like crust surface layer was formed during the gasification in nitrogen as seen in Fig. 12. Since the thermal conductivity of char is less than that of polymers, the surface temperature of the black crust layer would be significantly higher. Although it is not clear whether the surface temperature becomes high enough to generate significant chemical reactions among the residues and silica surface, solid phase NMR analysis of the residue samples of the PEO sample with silica gel collected at the end of the gasification test in nitrogen was conducted to determine the chemical structure of the residue.

^{13}C and ^{29}Si NMR measurements of the heat exposed PEO/SiO_2-gel residue collected at the end of the gasification test were made using a Bruker Avance 300 spectrometer operating at 75.47 MHz for ^{13}C, 59.63 MHz for ^{29}Si,

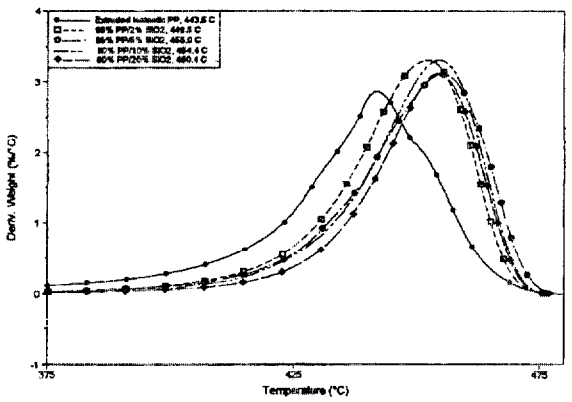

Figure 13. Derivative thermal gravimetric analysis of PP samples with various loading levels of silica gel in nitrogen at heating rate of 5°C/min. The temperatures in the legend are peak temperatures where the mass loss rate is at the largest.

and 300.13 MHz for ^{1}H under the condition of magic-angle-spinning (MAS) of 5 kHz. Figure 15 shows ^{29}Si and ^{13}C (Fig. 15c) solid-state NMR spectra of PEO/SiO_2-gel char. The ^{29}Si CPMAS spectrum (Fig. 15a) shows that three peaks appear at around -90, -100 and -110 ppm. These peaks are easily assigned to the Q2, Q3 and Q4 species of SiO_2, respectively.[12] Here Qi represents the number of siloxane bridges bonded to the silicon atom. The ^{29}Si spectrum of Fig. 15b is observed by single-pulse. There is a large difference in intensities among Q2 to Q4 between the spectra a and b. The relative proportions of these species in the spectrum a, which are obtained by least-squares fitting with a gaussian line shape, are about 11:45:44 for Q2:Q3:Q4, while those in b are 8:16:76. This indicates that the peak intensities of Q2 and Q3 increase largely via ^{1}H-^{29}Si cross-polarization. Since the relative intensity obtained from the cross-polarization experiment depends on the degree of proximity from a proton nucleus, these observations suggest that the Q2 and Q3 species have one or two Si-O-H instead of Si-O-Si. The spectrum of the original PEO sample with silica gel consists of Q3 and Q4 (21:79 not shown). Although the formation of Q2 is recognized in the heat exposed residue, no additional new peaks were observed from the heated residue.

The ^{13}C CPMAS spectrum in Fig. 15c shows the peak at 127 ppm attributed to polyaromatic carbons with small quantities of residual methyl and methylene carbons at the peaks of 18 ppm and 35 ppm, respectively. The polyaromatic carbons are thermally stable and critical ingredients in the formation of char.[13] These NMR results indicate that no significant reactions between carbons and silica occurred to form Si-O-C bonds and others. Therefore, the observed reduction in the mass loss rate of PEO samples by the addition of silicas appear to

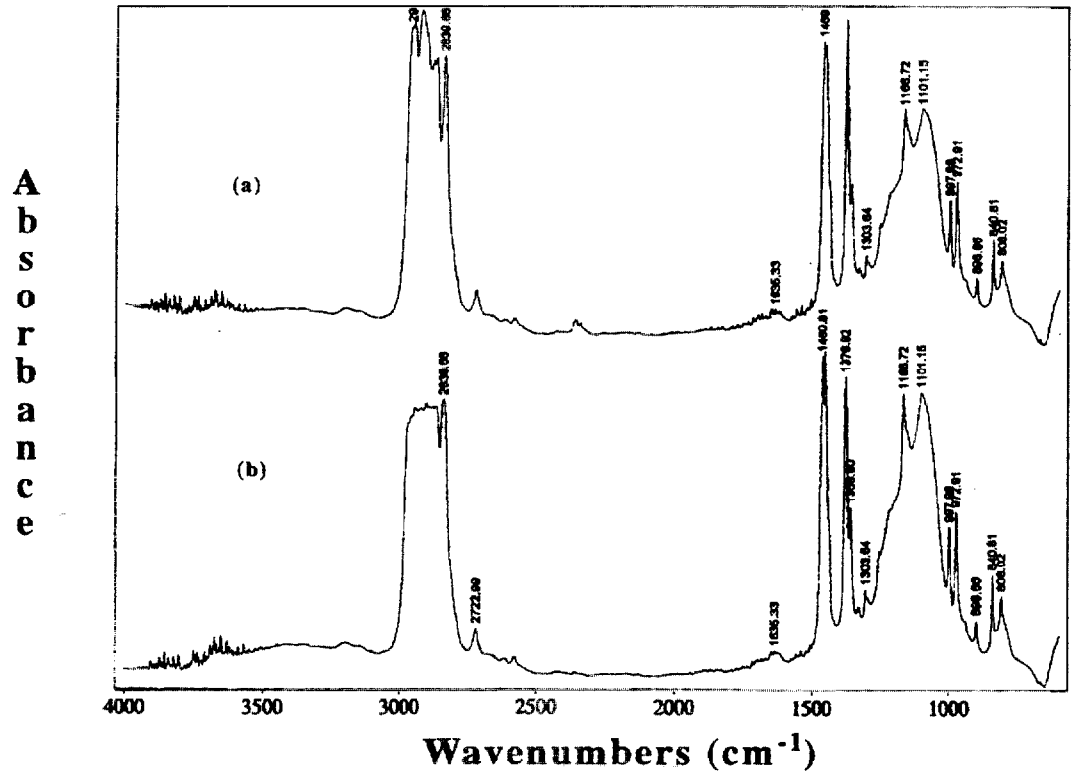

Figure 14. Comparison of FTIR spectra of PP with silica gel (mass fraction of 10%) original un-pyrolysed sample (a) and heated residue sample (b).

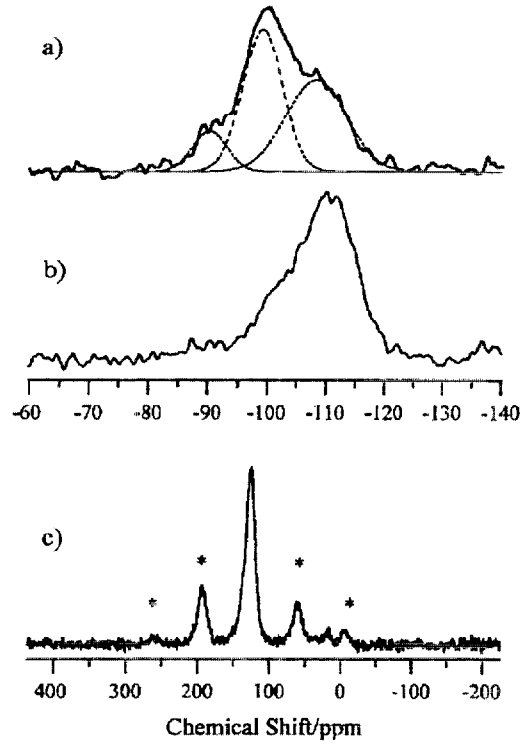

Figure 15. ^{29}Si and ^{13}C solid-state NMR spectra of the heated residue of PEO with silica gel collected at the end of the gasification test in nitrogen. (a) ^{29}Si CPMAS spectrum; (b) ^{29}Si single-pulse spectrum; (c) ^{13}C CPMAS spectrum, The asterisks indicate the artificial signal of spinning-side-band. Exponential window-function of 50 Hz was applied to all spectra.

be mainly due to physical processes instead of chemical processes.

The video images of the PP samples with silica gel show the formation of a solid-like surface layer during their gasification in nitrogen, posing the questions, what does this layer consist of, and also where are the silica gels or other silica particles during gasification? In order to answer these questions, we evaluated the accumulation of silica at the sample surface during gasification tests with the PP samples with silica gel (10% mass fraction). This was accomplished by measurement of the silicon concentration at the top layer of residues collected at different times. Five samples were collected: unheated, 185 s, 300 s, 500 s and 875 s. The silicon concentration in the collected samples was measured by neutron activation analysis at Dow Chemical Company. The results are shown in Fig. 16, with the corresponding mass loss rate curve. The Si concentration of the surface layer continued to increase with the exposure time due to accumulation of silica gel during continued degradation and gasification of PP. When the silica mass fraction exceeded about 20% (estimated from the Si concentration curve at about 250 s), the mass loss rate decreased significantly, but was followed by an increase due to an accumulation of heat in the sample despite a continued increase in silica at the surface layer. The silicon concentration in the sample increased to about ten times the initial value, and it is expected that the residue consisted mainly

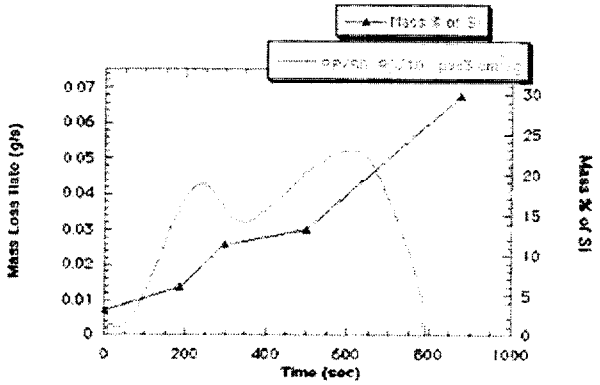

Figure 16. Mass loss rate curve and Si concentrations of the top layer of the five collected sample residues from the gasification of PP with silica gel (10% mass fraction) in nitrogen at 40 kW m^{-2}.

of silica at the end of the test because no char formation was observed as described above. The weight of the residue at the end of the test was about 8% to 9% of the original weight, so it appears that a small fraction of silica gel might be carried away into the gas phase during the tests.

The accumulation of silica near the surface during the gasification of PP has two important effects on the mass loss rate in nitrogen; one is the depletion of PP near the sample surface and the other is the formation of a thermal insulation layer. The latter effect has been clearly demonstrated by the measurement of heat transfer rate through various silica ash layer thickness. A reduction of roughly 65% of incident radiant flux was reported with a 1.5 mm thick of silica ash layer.[14] There could be various accumulation processes of silica particles. The variation is how silica particles correspond to the voids created by the evolved PP in the mixture of PP and silica particles. One extreme case is that silica particles do not fill the voids even as PP continues to degrade and do not recede during the gasification. At the end of this test, the thickness of the sample residue is the same as the initial thickness of the sample and consists of silica particles only and the density of the residue is that of the accumulated silica particles. The thicker silica accumulation layer has a better insulation performance.[14] If silica particles instantaneously fill the voids, the thickness of the sample residue decreases with the progress of the gasification. Silica particles accumulate near the regressing surface by sinking with the regressing PP. At the end of this test, the thickness of the sample residue is much thinner than the initial thickness of the sample. This concept of a change of the volume of the additives during the gasification of a polymer was first proposed in the recent theoretical study by Staggs.[15] His definition of the maximum change of volume of an inert additive is the case in which the additive instantaneously fills the voids, and his definition of no volume change is defined as the case in which the additive does not fill any of the voids. His theoretically calculated results indicate that the mass loss rate decreases with a smaller change in the volume of an inert additive. Since his study shows the results of high loading levels of inert additives (20%, 40%,

60% and 80% mass fraction), we calculated the case with the maximum change of the volume of silica particles (the most conservative case, instantaneously filling the voids) for the loading levels of silica gel used in this study.

Our model is basically the same as his model and it solves the one dimensional heat transfer equation through the polymer sample with a well-distributed inert additive with the boundary conditions corresponding to those used in the experiment. The degradation reaction of PP is distributed in the sample, and it is assumed that the degradation products leave the sample instantaneously. The kinetic constants used for a one-step, global, first- order Arrhenius equation were determined from a detailed study based on a molecular dynamic model,[16] and the results obtained from this study were used without any modification. The thermal properties of silica gel were taken to be the same as those of PP in this calculation to determine only the effects on mass loss rate by the depletion of PP with accumulation of silica gel near the sample surface. It is assumed that the incident external thermal radiation is absorbed at the sample surface. The calculated mass loss rate curves with different silica gel loading levels are shown in Fig. 17. The results indicate a significant reduction in mass loss rate with an increase in loading level of silica gel. This is due to the reduction of PP concentration near the regressing surface by an accumulation of silica gel and also to an increase of re-radiation from elevated surface temperatures. The surface temperature increases with the loading level of silica gel because the distance between the surface and the availability of PP increases with the loading level. (Since the thermal properties of silica gel are taken to be the same as those of PP in this calculation, thermal insulation effects are not included in this calculation.) The curves seen in Fig. 17 are very similar to those in Fig. 8, except for the mass loss rate trends at early exposure times and a larger reduction in experimentally measured mass loss rate than the calculated results. These trends at early exposure times are (1) mass loss begins too early in the calculation and (2) the addition of silica gel enhances early mass loss rate. The first discrepancy could be explained by the assumption of the absorption of the incident thermal radiation at the surface instead of a more realistic in-depth absorption, and the second discrepancy and the experimentally observed larger reduction in mass loss rate could be the difference in thermal properties between PP and silica gel. Stagg's results show an enhanced mass loss rate with the addition of an inert additive when the thermal conductivity of the additive is much lower than that of a polymer.[15]

Another question is why the addition of fused silica to PP and PEO is much less effective in reducing the mass loss rate compared with the addition of an equal loading of silica gel or fumed silica. In order to answer this question, the four gasification tests (PP with silica gel and fused silica and PEO with silica gel and with fused silica, all 10% mass fraction loading) were interrupted at specified times to collect the sample residues and to observe their surfaces. The pictures of the collected samples are shown in Fig. 18. The surface of the residue for PP with silica gel (Fig. 18a) is covered by silica gel and is opaque, indicating the accumulation of silica gel as observed

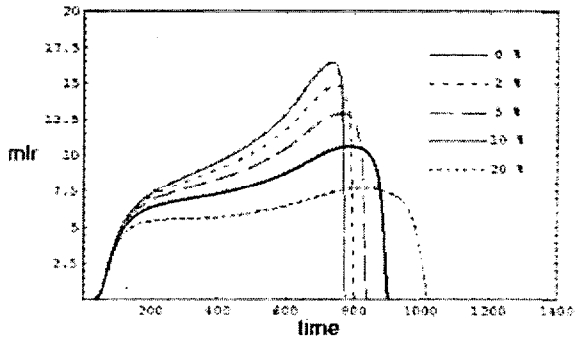

Figure 17. Calculated mass loss rate (mlr) (g/m²s) of PP with various loading levels of an inert additive in nitrogen at 40 kW m⁻².

previously. However, the surface of the residue of PP with fused silica (Fig. 18b) is translucent, and it appears that a majority of fused silica particles are below the surface. The surface of the residue of PEO with silica gel (Fig. 18c) is black and smooth with fine grain texture but the surface of the residue of PEO with fused silica (Fig. 18d) is a shiny, solidified polymer melt layer without many silica particles. Since the fused silica particles used in this study are dense fine particles, it appears that they do not accumulate near the regressing sample surface, but instead tend to sink through the molten polymer layer. Thus they do not reduce availability of polymer near the sample surface to slow down degradation of the polymer. It appears that the balance between the density of an inert additive and the melt viscosity of the polymer in which it resides determines whether the additive accumulates near the surface to slow down the degradation of polymer and form a thermal insulation layer. The smallest reduction of mass loss rate by the additive volume is therefore the case in which the heavy additives sink farther into the interior of the polymer melt layer when the melt viscosity of the polymer melt is low. Therefore, low density, fluffy, large surface area inert additives are the most effective for the reduction of mass loss rate (burning rate). The large surface area of the additive tends to increase polymer melt viscosity, and this tends to enforce accumulation of the additive near the surface. The only slight drawback of the low density, large surface area additives having low thermal conductivity is a minor reduction of ignition time and a small heat release rate increase at an early time. However, heavy, small surface-area additives are the least effective for reducing mass loss rate because they do not accumulate near the sample surface but instead sink through a polymer melt layer having a low melt viscosity. This conclusion is opposite from one of the conclusions described in the Staggs' paper[15] because sinking of the additive farther than the voids has not been recognized previously, and consequently was not included in his model.

The loading level of silica gel in PP affected the residue structure at the end of the gasification test. The residue of the PP sample with 2% mass loading of silica gel is in the form of powders which are left at the bottom of the pan. The residue of the PP sample with a 5% mass loading consists of a powder and patchy islands of compacted

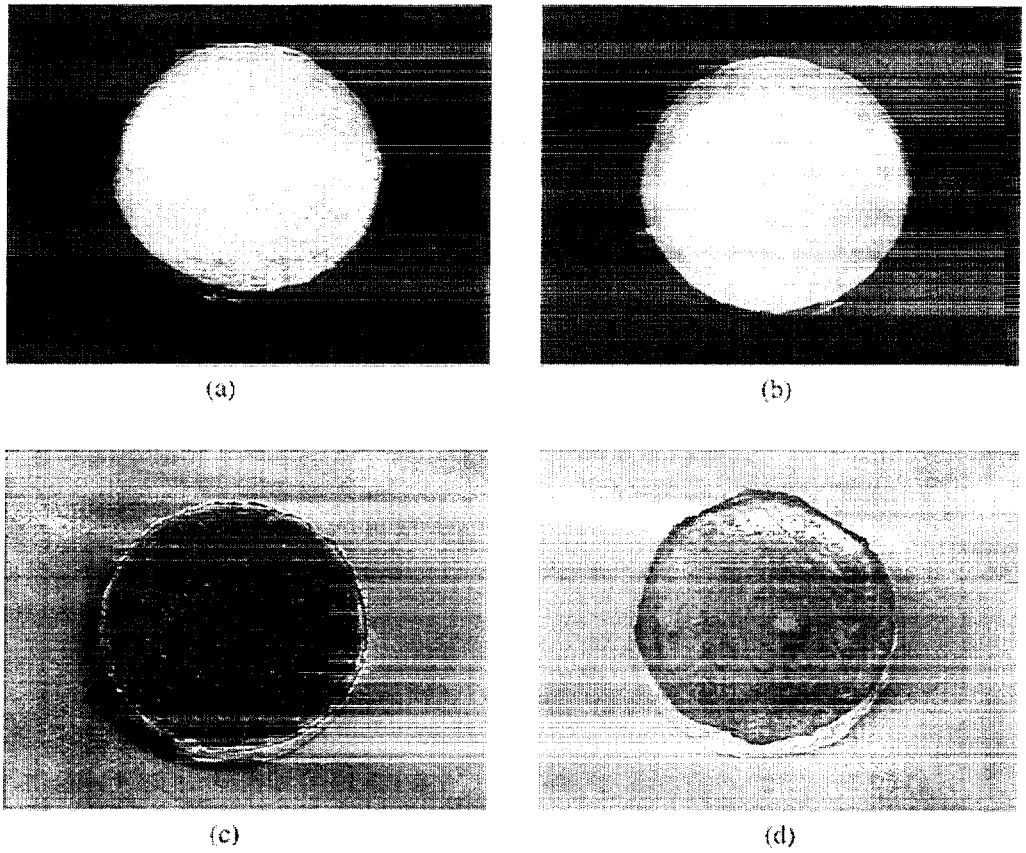

Figure 18. The pictures of the surfaces of the sample residues collected at specified time at 40 kW m $^{-2}$ in nitrogen. (a) PP with silica gel at 350 s, (b) PP with fused silica at 350 s, (c) PEO with silica gel at 250 s, and (d) PEO with fused silica at 250 s. The loading level of silica is at 10% mass fraction.

silicas such as seen in Fig. 9. The residue was at the bottom of the pan at the end of the gasification test. The sample surface of the 10% mass loading is initially covered by powder such as seen in Fig. 16(a) but patchy islands of compacted silicas gradually form and the residue at the end of the test is mainly in the form of islands. The thickness of the residue is greater than those of 2% and 5% mass loading samples but much less than the initial sample thickness. However, the thickness of the residue of the PP sample with 20% mass loading is slightly thicker than the initial sample thickness and it is in the form of the silica compacted islands as seen in Fig. 9. Therefore, the concept of a change in volume of an inert additive proposed by Staggs is reasonable for describing the physical phenomena of the behavior of these additives, but two additional factors should be included: the effect of polymer melt viscosity, and sinking of heavy, low surface area additives.

CONCLUSION

The addition of various types of silicas to PP and PEO reduced the heat release rate and burning rate as measured in the cone calorimeter, and also the mass loss rate as measured in the nitrogen gasification device. The heat release and the mass loss rate of PP decreased nearly inversely with the mass loading level of silica gel up to a 20% mass fraction. The mechanism of the reduction in the heat release rate and mass loss rate is due to physical processes in the condensed phase. Fumed silicas and silica gel having a large surface area and low density significantly increased the polymer melt viscosity of PP and PEO during their gasification/burning. Consequently the additives accumulated near the regressing sample surface without sinking through the polymer melt layer. The accumulated silica acted as an insulation layer and possibly as a barrier to the transport of degradation products to the surface. The accumulated silica reduced the concentration of PP and PEO near the surface. The reduction in heat release rate and mass loss rate are mainly due to these reasons. However, a heavy, and low surface area additive such as the fused silica used in this study tended to sink through the polymer melt layer during the gasification process and was not effective in reducing the heat release rate and mass loss rate. The effectiveness of the inert additive depended on the balance between the density and surface area of the additive and polymer melt viscosity, controlling the accumulation of the silica layer near the sample surface. PEO samples with fumed silicas and silica gel form physically strong char/silica surface layers. These layers acted not only as thermal insulation to protect virgin polymer, but also

acted as barriers against the migration of the thermal degradation products to the surface. The latter was confirmed by swelling of the sample and, sometimes, subsequent development of a large crack through the char/silica layer.

Acknowledgement

A part of this study was funded by the Industrial Consortium on Flame Retardant Mechanism of Silica Gel. Authors are grateful to Dow Chemical Co. for the Si analysis and to Dr David L. VanderHart for the interpretation of the NMR spectra.

REFERENCES

1. Lyons J W. *The Chemistry and Uses of Fire Retardants.* Wiley-Interscience: New York, 1970.
2. Gilman J W, Ritchie S J, Kashiwagi T, Lomakin S M. *Fire Mater.* 1997; **21**: 23–32.
3. Gilman J W, Kashiwagi T, Lichtenhan J D. *SAMPE J* 1997; **33**: 40–46.
4. Gilman J W, Kashiwagi T, Nyden M *et al. Chemistry and Technology of Polymer Additives,* Al-Malaika S, Golovoy A, Wilkie CA (eds). Blackwell Science: Oxford, 1999, ch 14.
5. Gilman J W, Lomakin S, Kashiwagi T, VanderHart D L, and Nagy V. *Fire Mater.* 1998; **22**: 61–67.
6. Gilman J W, Kashiwagi T, Nyden M, Harris R H Jr. *New Flame Retardants Consortium: Final Report-Flame Retardant Mechanism of Silica, NISTIR* 6357, June 1999.
7. Austin P J, Buch R R, Kashiwagi T. *Fire Mater.* 1998; **22**: 221–237.
8. *"Cab-O-Sil Untreated Fumed Silica Properties and Functions"* Cabot Corp. TD-100, May 1997.
9. Wypych G. *Hand Book of Fillers,* 2nd edn. Chemical Technology Publishing: Toronto, 1999; ch 2.
10. Iler R K. *The Chemistry of Silica.* John Wiley & Sons: New York, 1979; 588.
11. Tsagaropoulos G, Eisenberg A. *Macromolecules* 1995; **28**: 6067–6077.
12. Hajji P, David L, Gerard J F, Pascault J P, Vigier G. *J Polym Sci Part B: Polym Phys* 1999; **37**: 3172–3187.
13. Factor A. *Fire and Polymers,* Nelson GL (ed.), ACS Symposium Series 425. ACS: Washington, DC, 1990; 274–287.
14. Hshieh Fu-Yu *Fire Mater* 1998; **22**: 69–76.
15. Staggs J E J. *Fire Safety J* 1999; **32**: 221–240.
16. Nyden M R. *International Aircraft Fire and Cabin Safety Research Conference,* November 16–20, Atlantic City, NJ. 1998.